Mineralogical Magazine, April 2000, Vol. 64(2), pp. 291–300

A high temperature structural phase transition in crocoite ($PbCrO_4$) at 1068 K: crystal structure refinement at 1073 K and thermal expansion tensor determination at 1000 K

K. S. KNIGHT*

ISIS Facility, CLRC Rutherford Appleton Laboratory, Chilton, Didcot, Oxfordshire, OX11 0QX, and Department of Mineralogy, Natural History Museum, Cromwell Road, London SW7 5BD, UK

ABSTRACT

High-resolution, neutron time-of-flight, powder diffraction data have been collected on natural crocoite between 873 and 1073 K. Thermal analysis carried out in the 1920s had suggested that chemically pure $PbCrO_4$ exhibited two structural phase transitions, at 964 K, to the β phase, and at 1056 K, to the γ phase. In this study, no evidence was found for the α–β structural phase transition, however a high-temperature phase transition was found at ~1068 K from the ambient-temperature monazite structure type to the baryte structure type. The phase transition, close to the temperatures reported for the β to γ phase modifications, is first order and is accompanied by a change in volume of −1.6%. The crystal structure of this phase has been refined using the Rietveld method to agreement factors of $R_p = 0.018$, $R_{wp} = 0.019$, $R_p = 0.011$. No evidence for premonitory behaviour was found in the temperature dependence of the monoclinic lattice constants from 873 K to 1063 K and these have been used to determine the thermal expansion tensor of crocoite just below the phase transition. At 1000 K the magnitudes of the tensor coefficients are α_{11}, $2.66(1) \times 10^{-5}$ K^{-1}; α_{22}, $2.04(1) \times 10^{-5}$ K^{-1}; α_{33}, $4.67(4) \times 10^{-5}$ K^{-1}; and α_{13}, $-1.80(2) \times 10^{-5}$ K^{-1} using the IRE convention for the orientation of the tensor basis. The orientation of the principal axes of the thermal expansion tensor are very close to those reported previously for the temperature range 50–300 K.

KEYWORDS: crocoite, phase transition, neutron diffraction, thermal expansivity.

Introduction

SYNTHETIC $PbCrO_4$ is known to be dimorphous from X-ray powder diffraction investigations of precipitated salts from aqueous solutions containing Pb^{2+} (Wagner, 1931; Wagner *et al.*, 1932; Quittner *et al.*, 1932). Crocoite, the natural monoclinic polymorph, was found to be precipitated from aqueous solutions of K_2CrO_4 and $Pb(CH_3COO)_2$, whereas an orthorhombic phase was produced from solutions of $Pb(NO_3)_2$ with K_2CrO_4. Somewhat surprisingly a crystal structure for the orthorhombic phase was proposed first (Collotti *et al.*, 1959) even though large untwinned crystals of crocoite exist in nature. The powder diffraction pattern showed that the orthorhombic polymorph was isostructural to baryte, space group *Pnma*, and trial coordinates were refined using an early example of pattern decomposition. The crystal structure of crocoite was determined independently by Quareni and de Pieri (1964, 1965) and Náray-Szabó and Argay (1964) using X-ray Weißenberg data following on from the much earlier work of Brody (1942) who determined approximate cation positions using Patterson synthesis. These works showed that crocoite was isostructural with monazite, monoclinic space group $P2_1/n$. The ambient-temperature unit-cell volume of the baryte isomorph is 1.6% less than that of crocoite suggesting that it might have been produced as a metastable phase from solution and may exist as a stable low-temperature or high-pressure phase. On the basis of this observation, the crystallography of crocoite

* E-mail: ksk@isise.rl.ac.uk

from 4.5 to 300 K has been studied by Knight (1996) using Rietveld analysis of high-resolution, neutron time-of-flight, powder diffraction data. This low temperature study has shown that crocoite does not undergo structural or magnetic phase transitions down to 4.2 K and that the crystal structure is barely altered throughout this temperature range.

According to thermal analysis and high-temperature X-ray powder diffraction, chemically pure $PbCrO_4$ exhibits two high-temperature structural phase transitions. The $\alpha-\beta$ phase transition temperature in $PbCrO_4$ has been reported as 964 ± 10 K by Pistorius and Pistorius (1962) using X-ray diffraction and as 980 K by Jaeger and Germs (1921) using thermal analysis. Jaeger and Germs characterized the phase transition as showing only a 'small thermal effect', and is presumably second order. However, they found no evidence for this transition in natural crocoite from the localities at Dundas, Tasmania and Beresowsk, Urals. Pistorius and Pistorius simply reported an unidexed and uncharacterized powder diffraction pattern collected *in situ* at 1003 K in the β phase and stated in their paper that it was not consisitent with either an anglesite (baryte structure, orthorhombic, space group *Pnma*) or wulfenite (tetragonal, space group $I4_1/a$) diffraction pattern. This phase was apparently quenchable to room temperature with degraded crystallinity. The $\beta-\gamma$ phase transition temperature was determined by Jaeger and Germs to occur at 1056 K in chemically pure $PbCrO_4$ and 1065 K in natural crocoite. It was characterized by a 'large thermal effect' and exhibited hysteresis suggesting it is first order in nature. Pistorius and Pistorius quenched a sample of $PbCrO_4$ from 1080 K and reported a diffraction pattern different from both crocoite and the β phase but were unable to determine whether this was indeed the γ phase or a decomposition product due to loss of oxygen from the sample. In order to shed light on some of the ambiguities of the structure of $PbCrO_4$ at high temperature we have carried out a high-resolution neutron powder diffraction investigation of natural crocoite from 873 to 1073 K.

Experimental, data reduction and normalization

A powder sample of crocoite (Dundas, Tasmania, ex B.M. No. 1913.380) was prepared by lightly grinding hand-picked, phase-pure, single crystal fragments in an agate pestle and mortar and sieving to <75 μm. The chemical composition of the sample is included in Table 4 and represents the average of 50 analyses measured on a Cameca SX50 wavelength dispersive microprobe operating at 20 kV, 20 nA with PbO, Mo, Cr and $SrSO_4$ as standards. Our previous attempt to carry out high temperature structural studies of crocoite had suffered from severe sample degradation at temperatures as low as 673 K. This chemical breakdown has been attributed to oxygen loss from the compound at high temperature (Parkes, 1952). This oxygen loss is further exacerbated by the requirement to run the sample and furnace under a vacuum using continuous pumping due to the use of both vanadium heating elements and shields, and hence for the experiment reported here, the sample was sealed in a lightly evacuated (10^{-3} mbar) quartz-glass ampoule (Ampoules manufactured by H. Baumbach & Co. Ltd., 30 Anson Road, Martlesham Heath, Ipswich, Suffolk IP5 7RG, England) to minimize this effect. Approximately 7 g of powder was loaded into the 10 mm diameter ampoule which was filled to a height of ~30 mm. The powder was then dried to prevent containment failure due to surface moisture being driven off at high temperatures, and the sample was isolated from the vacuum pump with a quartz-glass-wool plug before being sealed. The region of the ampoule intercepting the incident neutron beam was made from suprasil glass and had a wall thickness of 0.5 mm, the remainder of the ampoule was manufactured from quartz glass. The sealed ampoule was loaded into a deep-drawn, cylindrical, vanadium sample can of wall thickness 0.14 mm which was then mounted on the centre stick of the furnace. The centre stick was located in the furnace and the whole assembly was pumped down to a working pressure of 10^{-4} mbar before the heating of the sample commenced. The sample was heated to 373 K for 2 h to allow out-gassing from the walls of the furnace and the vanadium element to occur, and during the data collections reported here, the furnace ran at an average background pressure of 5×10^{-6} mbar. The sample and furnace temperatures were monitored using two type K thermocouples, one located 20 mm above beam centre and wired to the wall of the vanadium can, and the second in the centre of the furnace below the bottom of the can. Temperature variations on the sample can thermocouple were $< \pm 0.25$ K over all the data collections and the differences between the two thermocouples was always

<2 K. Diffraction patterns were collected in 25 K steps from 873 K up to 923 K and in 10 K steps thereafter as the temperature approached the published $\alpha-\beta$, and $\beta-\gamma$ phase transition temperatures.

Neutron time-of-flight data were collected at the ISIS spallation source on the high-resolution powder diffractometer HRPD (Johnson and David, 1985; Ibberson *et al.*, 1992) using the lower resolution 1m sample position. Data in the time-of-flight range 30–130 ms, binned logarithmically as $\Delta t/t = 1 \times 10^{-4}$, were used for the lattice constant study, and data from 50–150 ms were used for the Rietveld structure refinement of the high-temperature phase. Only the data collected in the high-resolution back-scattering detectors (resolution $\Delta d/d = 4 \times 10^{-4}$ over the whole pattern) were used in the subsequent data analysis and for this bank of detectors the conversion from time-of-flight (TOF) to lattice spacing is given by $d(\text{Å}) = 2.07339 \times 10^{-2}$ TOF(ms). Data collection times were 30 min per temperature for the lattice constant study and 11 h for the structure refineable data set. A 5 min temperature equilibration period was applied between each temperature step.

The data from the backscattering detectors were background subtracted, normalized to the incident flux spectrum using an upstream beam monitor, focused to a total flight path of 95.8918 m and a Bragg angle of 84.164° and corrected for the wavelength dependent detector efficiency using a spline-smoothed data set from a V standard. The empty furnace background was subtracted from the 30–130 ms data sets but not from the 50–150 ms data as there was insufficient time to collect these data. To produce a file for profile analysis, the data were then corrected for the wavelength dependent absorption in the furnace windows and finally re-binned with $\Delta t/t = 3 \times 10^{-4}$, which corresponded to the required resolution for the sample.

Results

Lattice constant refinement

The results from a room temperature neutron powder diffraction structure refinement of natural crocoite (Knight, unpubl.) were used as a basis for the determination of the lattice constants from 873 to 1069 K. Profile refinement at each temperature was carried out by varying scale, background, peak shape, coordinates and a global temperature factor for all atoms. For a typical refinement, e.g. the 973 K data collection, the agreement factors were $R_p = 8.5$, $R_{wp} = 8.9$, $R_E = 9.1$ and gave lattice constant precisions of ~2 parts in 70000.

The diffraction data were carefully monitored from 933 to 1013 K to search for evidence of the $\alpha-\beta$ phase transition. No evidence was found for either a change in the diffraction pattern such as the disappearance, appearance or merging of diffraction peaks and no discontinuities in the temperature dependence of peak intensities or lattice constants were observed within this temperature range. These observations, in agreement with the thermal analysis results of Jaeger and Germs (1921), provide further evidence that this transition is absent in natural crocoite.

The diffraction data showed no evidence for structural change up to 1063 K. However, at 1073 K new diffraction maxima were observed. As the whole diffraction pattern is collected simultaneously in a time-of-flight experiment, the growth of the high temperature phase could be followed by collecting and suspending the data collection periodically. The structural change from the low temperature phase to the high temperature phase was found to be complete within 30 min and after this time there was no evidence for the monoclinic phase. The effect of the Debye-Waller factors and thermal diffuse scattering had removed all the high Q data ($Q = 4\pi\sin(\theta)/\lambda$) at this temperature, and hence the time-of-flight window was re-phased to 50–150 ms to collect a data set suitable for profile refinement in this phase. To aid unit-cell determination, a further data set was collected at 1073 K with the time-of-flight window re-phased to 130–230 ms.

The results from the lattice constant refinements are given in Table 1 and plotted in Fig. 1. There was no evidence for premonitory behaviour in any of the lattice constants, all showing a linear trend with temperature for 873 K $\leqslant T \leqslant$ 1063 K, and as a result have been fitted to an equation of the form $p = p_0(1 + kT)$. The values of p_0 and k with their associated esd's are reported in Table 2. The equivalent coefficients recalculated from the results of Pistorius and Pistorius (1962) are included for comparison.

On the basis of the simple linear behaviour of the unit cell dimensions with temperature, the thermal expansion tensor has been calculated for a temperature of 1000 K. The calculation has been carried out using the Lagrangian form of the thermal expansion tensor given by Schlenker *et al.* (1975), but transforming the basis to the IRE

TABLE 1. Lattice constants of crocoite between 873 and 1073 K.

T (K)	a (Å)	b (Å)	c (Å)	β (°)
873	7.23427(3)	7.51720(3)	6.92288(3)	103.3552(3)
898	7.23980(8)	7.52119(8)	6.92959(7)	103.3956(8)
923	7.24565(7)	7.52511(8)	6.93679(7)	103.4374(8)
933	7.24797(8)	7.52668(8)	6.93964(7)	103.4550(8)
943	7.25037(8)	7.52805(8)	6.94272(7)	103.4746(8)
953	7.25263(8)	7.52966(8)	6.94562(7)	103.4916(8)
963	7.25492(8)	7.53115(9)	6.94857(7)	103.5084(8)
973	7.25747(8)	7.53285(9)	6.95150(8)	103.5262(9)
983	7.25976(8)	7.53435(9)	6.95465(8)	103.5447(9)
993	7.26235(9)	7.53595(9)	6.95772(8)	103.5616(9)
1003	7.26476(9)	7.53736(9)	6.96095(8)	103.5791(9)
1013	7.26719(9)	7.53914(9)	6.96410(8)	103.5997(9)
1023	7.26972(9)	7.54051(9)	6.96737(8)	103.6184(9)
1033	7.27230(9)	7.54200(9)	6.97071(8)	103.6367(9)
1043	7.27489(9)	7.54322(10)	6.97381(9)	103.6564(10)
1053	7.27743(9)	7.54482(9)	6.97745(8)	103.6743(9)
1063	7.27991(10)	7.54633(11)	6.98082(10)	103.6930(11)
1073	8.79861(4)	5.73422(2)	7.27402(3)	90.0

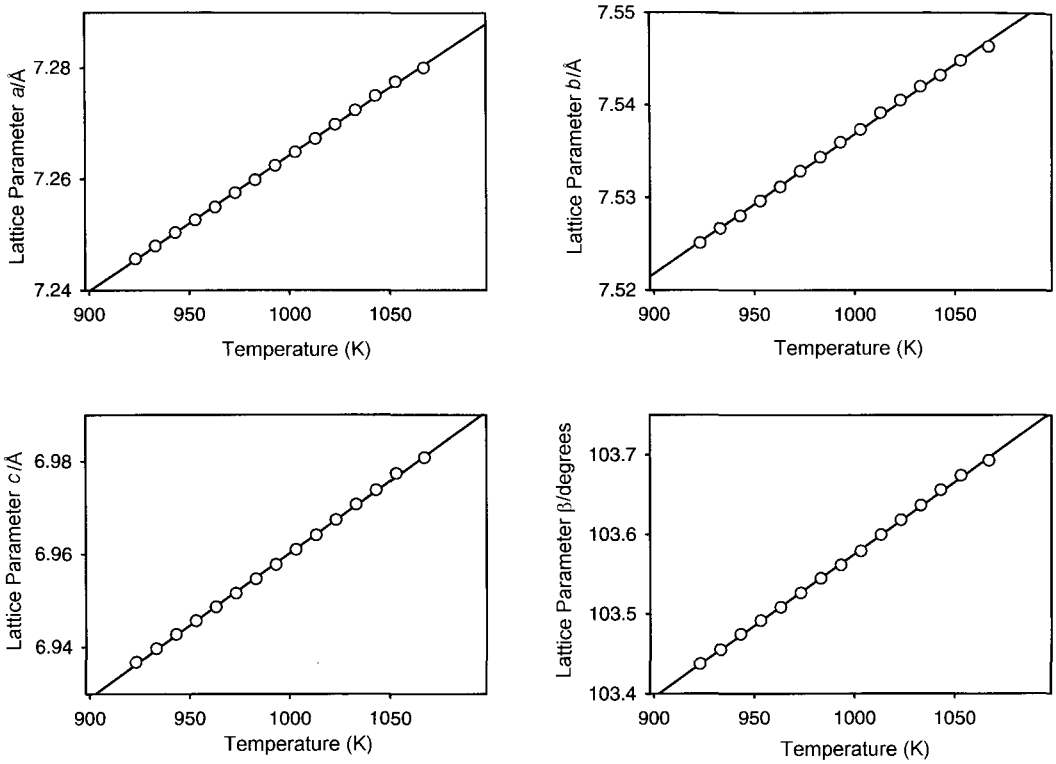

FIG. 1. Temperature dependence of the lattice constants of crocoite between 873 and 1073 K. Estimated standard deviations for each of the lattice constants are smaller than the plotting symbols used in each case. The calculated temperature dependence, given by the straight lines, was derived from least-squares fitting to the data.

TABLE 2. Lattice thermal expansion coefficients.

	a	*b*	*c*	β	*V*
Present study					
p_0	7.021(1) Å	7.386(1) Å	6.649(2) Å	101.77(1)°	336.9(2) Å^3
$\alpha/10^{-5}$	3.46(1) K^{-1}	2.04(1) K^{-1}	4.68(3) K^{-1}	1.77(2) K^{-1}	9.94(6) K^{-1}
Pistorius and Pistorius (1962)					
p_0	7.063 Å	7.384 Å	6.744 Å	102.24°	343.18 Å^3
$\alpha/10^{-5}$	2.62 K^{-1}	2.33 K^{-1}	2.55 K^{-1}	0.60 K^{-1}	7.73 K^{-1}

Estimated standard deviations in parentheses. All coefficients derived from linear regression analysis of lattice constants, $p = p_0 (1.0 + \alpha T)$. The results of Pistorius and Pistorius (1962), derived from two measurements at 293 and 883 K, are shown for comparison.

convention of $\mathbf{e_3} \| \mathbf{c}$, $\mathbf{e_2} \| \mathbf{b^*}$, $\mathbf{e_1} = \mathbf{e_2} \times \mathbf{e_3}$ (Jessen and Küppers, 1991). The thermal expansion tensor coefficients derived from the least squares fitting to the temperature dependence of the lattice constants are, α_{11}, $2.66(1) \times 10^{-5}$ K^{-1}; α_{22}, $2.04(1) \times 10^{-5}$ K^{-1}; α_{33}, $4.67(4) \times 10^{-5}$ K^{-1}; and α_{13}, $-1.80(2) \times 10^{-5}$ K^{-1}. By diagonalizing the tensor the magnitudes of the principal axes have been evaluated as α_{11}, $1.57(4) \times 10^{-5}$ K^{-1}; α_{22}, $2.04(1) \times 10^{-5}$ K^{-1}; α_{33}, $5.71(6) \times 10^{-5}$ K^{-1}, with $\alpha_{22} \| \mathbf{b}$ and α_{33} lying at 35.5° to **c**. The crystal structures of monoclinic crocoite viewed down each of the principal axes with the representation quadric superimposed are shown in Fig. 2.

The orientation of the tensor is close to that determined at 300 K by Knight (1996) in a study of the temperature dependence of the thermal expansion tensor of crocoite between 60 and 300 K. At 300 K the temperature dependence of the thermal expansion tensor appeared to saturate with principal axis magnitudes, α_{11}, $3.36(1) \times 10^{-6}$ K^{-1}; α_{22}, $1.572(3) \times 10^{-5}$ K^{-1}; α_{33}, $3.31(1) \times 10^{-5}$ K^{-1}; and α_{33} lying at 37.9° to **c**. The orientation of the maximum principal axis was found to be parallel to the least-squares line passing through the projection of the Cr atoms onto (010). A potential structural basis for this orientation was proposed as allowing the CrO_4 tetrahedra to rotate into the configuration that exists in the baryte structure.

Crystal structure refinement of the high temperature polymorph

Using both the time-of-flight windows, the twenty reflections with the highest *d*-spacings were evaluated and showed the unit cell metric to be orthorhombic and with magnitudes consistent with the baryte structure type. The estimated lattice constants and space group were subsequently confirmed using a Pawley (1981) refinement of the data. The refined lattice constants, background and peak-width parameters derived from this analysis were then held constant on the initial Rietveld analysis of the structural model using the coordinates of the X-ray structure of Collotti *et al.* (1959) as the starting parameters. The isotropic refinement converged rapidly to $\chi^2 = 6$ but showed the Pb atoms to be vibrating with $u_{iso} > 0.12$ Å^2. Although the temperature of the data collection is 96% of the absolute melting temperature of 1117 K (Jaeger and Germs, 1921), the magnitude of the isotropic thermal parameter seemed to be excessive and a disordered model with the Pb atoms displaced from the mirror plane was attempted. This model also converged with large isotropic displacement parameters and attempts were then made to improve the refinement on introducing anisotropic displacement parameters for the Pb atom which was successful. The most significant improvement to the fit however was derived by introducing anisotropic displacement parameters for the anions. The χ^2 reduced by 50% and assessment of the refined values showed thermal motion to be perpendicular to the Cr–O bonds as would be expected for isolated tetrahedra. The refinement converged at $R_p = 1.8\%$, $R_{wp} = 1.9\%$, $R_E = 1.1\%$ with the fit to the data being shown in Fig. 3, and the crystal structure in Fig. 4. It should be noted that the agreement factors are low, principally because of the magnitude of the background which arises from both the unsubtracted furnace background for this time-of-flight window and

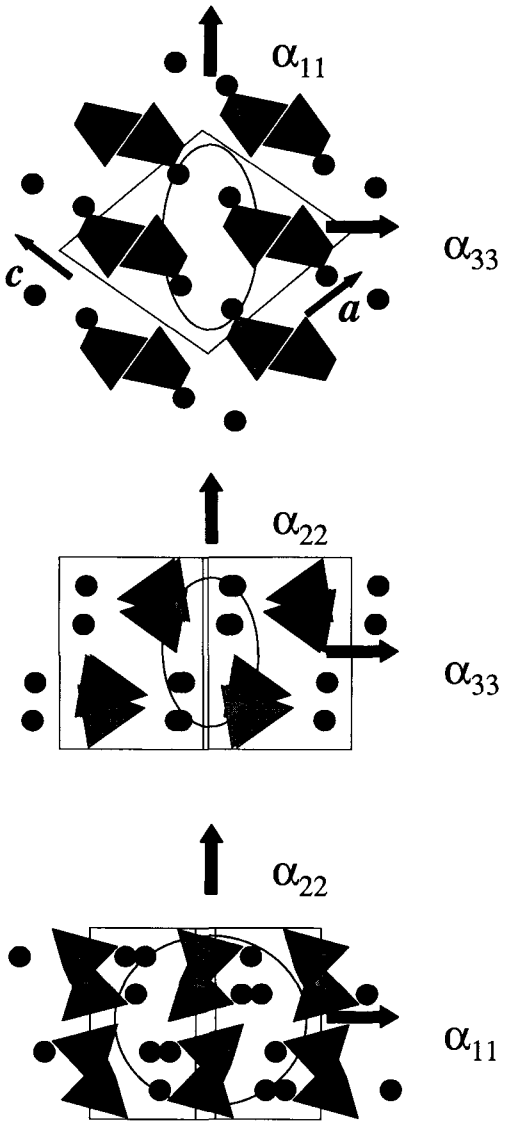

FIG. 2. The representation quadric of the thermal expansion tensor for crocoite viewed down each principal axis superimposed on the crystal structure in the $P2_1/n$ setting measured at 873 K (Knight, unpubl.).

thermal diffuse scatter. The structural parameters are reported in Table 3 with a summary of the refinement details in Table 4. The bond distances in the coordination polyhedra, uncorrected for thermal motion, are given in Table 5 where they are compared to the room temperature crocoite refinement of Knight (unpubl.).

Discussion and conclusions

Crocoite has been found to undergo a high-temperature structural phase transition at ~1068 K from the ambient-temperature monazite structure to the baryte structure type. Although we had insufficient time to monitor the transition on a cooling cycle, the phase transition is clearly reversible as a room-temperature neutron diffraction pattern showed the monoclinic crocoite phase without any evidence of the degraded crystallinity observed by Pistorius and Pistorius (1962). A phase transition from the monazite to the baryte structure type has been observed previously by Popovkin and Simanov (1962) to occur in $PbSeO_4$ at 918 K, but for this compound, the transition was found to be irreversible.

Comparison of the thermal expansion tensor at 1000 K with that determined at 300 K (Knight, 1996) shows only small differences in the orientation of the principal axes although there is a significant increase in the magnitudes from the apparently saturated values based on the 0 K lattice parameters, Einstein constants and Einstein temperatures. The conclusion made by Knight (1996) on the basis of the low-temperature investigation, that the principal axes were not related to the lattice constants of the orthorhombic phase, has been verified in this study. Despite the group–subgroup relationship that exists between the two space groups, the phase transition is first order and reconstructive. There is a however a strong similarity between the two structure types as can be seen in Fig. 5. Quareni and de Pieri (1965) were the first to show the similarity in coordination in both structures around a centre of symmetry where the principal difference between the two structures lies in the orientation of the CrO_4 tetrahedra which requires only modest displacements and rotations to move from the monazite to the baryte structure type. Knight (1996) suggested that as the largest principal axis of the thermal expansion tensor lay approximately parallel to the least squares line passing through the projection of the chromium atoms on (010), it was possible that the phase transition to the baryte structure type occurred due to the increasing separation of the Cr atoms allowing large, rigid unit librations of the chromate group into the required orientation.

The similarity between the structures is certainly suggestive of such a mechanism. However, there are some aspects of the refined structure that require comment and further work.

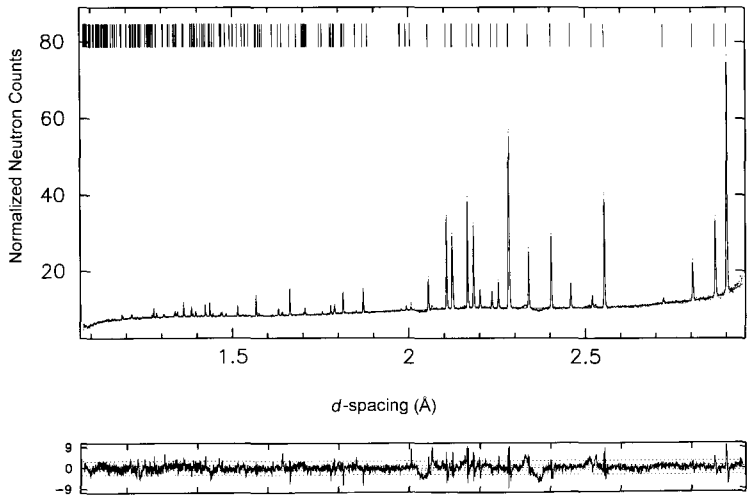

FIG. 3. Rietveld fit to crocoite at 1073 K in the baryte modification.

The magnitudes of the anisotropic displacement parameters for the anions are sufficiently large that the whole tetrahedron may in fact be rotationally disordered, a possibility which we have not been able to test due to the lack of a spherical harmonic expansion in the Rietveld refinement we used. If the tetrahedron was rotationally disordered we might expect to see modulations in the background which we have not observed on the HRPD data. Unfortunately the

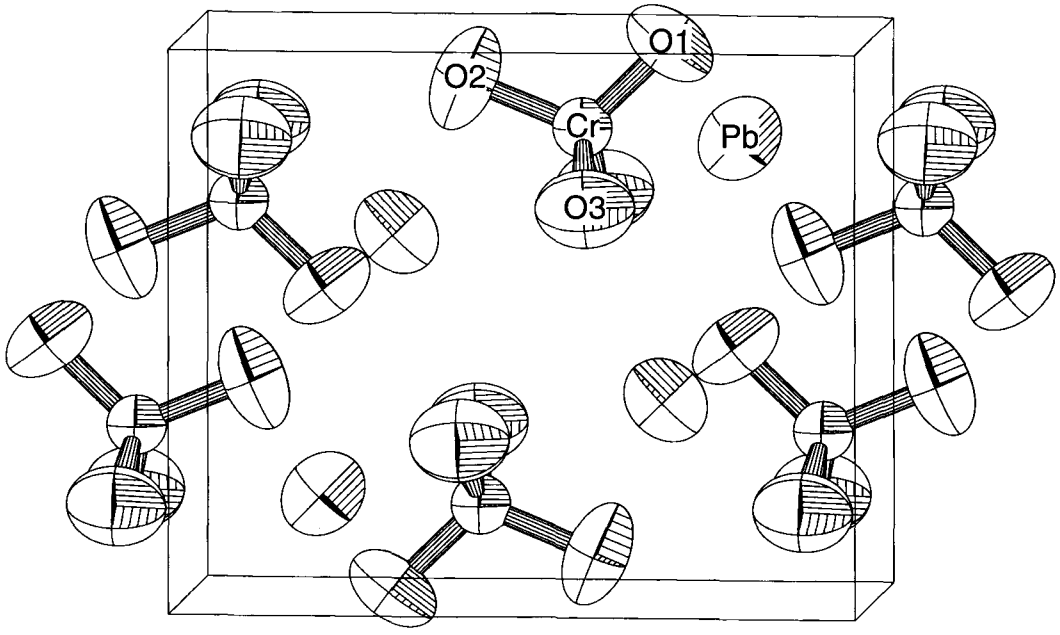

FIG. 4. The crystal structure of crocoite at 1073 K in the baryte-structured phase. Thermal ellipsoids are shown at 50% probability.

TABLE 3. Structural parameters for crocoite at 1073 K.

Atom	x	y	z	100 U_{eqv} (Å^2)
Pb	0.1817(3)	0.2500	0.1641(4)	12.9(3)
Cr	0.0592(6)	0.2500	0.6824(8)	6.1(1)
O1	0.1882(5)	0.2500	0.5338(6)	13.4(4)
O2	0.8897(4)	0.2500	0.5974(6)	14.7(5)
O3	0.0772(4)	0.0150(6)	0.8121(5)	12.8(3)

nature of a low repetition-rate chopper diffractometer coupled with the short wavelength cut-off of a neutron guide precludes gaining data with a wide enough range in Q using HRPD to observe these modulations if they do occur. Neutron diffraction data collected at medium resolution with a sealed 'null-scattering' sample can (to avoid modulations arising from a glass ampoule), may well be better suited to investigate the detailed structure of the baryte polymorph and to allow an atomistic model for the phase transition to be proposed. Furthermore, data collected on a higher flux instrument, with a wider accessible range in Q, might allow assessment of anharmonic effects which would be expected to occur at 96% of the absolute melting temperature.

On the basis of the measurements we have made, it is not possible to speculate on why Jaeger

TABLE 4. Data collection and refinement parameters for crocoite at 1073 K.

Instrumental	
Diffractometer	HRPD, neutron time-of-flight powder diffractometer
Flight path	95.8918 m
Detector	^{6}Li-doped ZnS scintillation counters, 168.329°2θ
Sample position	1 m
Data range	50000–150000 μs time-of-flight
Time channel binning	$\Delta t/t = 1 \times 10^{-4}$
Experiment duration	~11 h
Temperature	1073 K
Sample	
Compound	crocoite, $PbCrO_4$, (BM No. 1913.380)
Chemical Composition (Weight %)	PbO 69.79(45), CrO_3 30.29(46), MoO_3 0.08(6) SO_3 0.17(4), Σ100.33
Molecular weight	323.18
Density, calculated	5.85 gcm^{-3}
Refinement	
Space Group	*Pnma*
Z	4
Unit cell (Å)	a = 8.79861(4), b = 5.73422(2), c = 7.27402(3)
Unit cell volume (Å^3)	366.997(2)
Observations	3350
Refined parameters	
structural	30
profile/background	3/10
Unit cell	3
Thermal parameters	Cr, isotropic, Pb and O, anisotropic.

TABLE 5. Selected bond lengths and angles for crocoite at 1073 and 293 K.

293 K			1073 K			
Atom 1	Atom 2	Distance (Å)	Atom 1	Atom 2	Distance (Å)	No. of bonds
Pb	O1	2.646(4)	Pb	O1	2.689(6)	2
Pb	O1	2.537(3)	Pb	O2	2.640(5)	2
Pb	O2	3.078(3)	Pb	O3	3.036(5)	2
Pb	O2	2.559(3)	Pb	O3	2.744(4)	2
Pb	O2	2.804(3)	Pb	O3	2.823(4)	2
Pb	O3	2.684(3)				
Pb	O3	2.613(3)				
Pb	O4	2.684(3)				
Pb	O4	2.564(3)				
Cr	O1	1.654(5)	Cr	O1	1.569(6)	
Cr	O2	1.664(5)	Cr	O2	1.615(5)	
Cr	O3	1.665(5)	Cr	O3	1.652(4)	2
Cr	O4	1.642(5)				

293 K				1073 K				
Atom 1	Atom 2	Atom 3	Angle (°)	Atom 1	Atom 2	Atom 3	Angle (°)	No. of angles
O1	Cr	O2	108.8(2)	O1	Cr	O2	113.9(4)	
O1	Cr	O3	111.8(3)	O1	Cr	O3	108.9(3)	2
O1	Cr	O4	105.8(3)	O2	Cr	O3	107.9(3)	2
O2	Cr	O3	107.0(2)	O3	Cr	O3	109.3(4)	
O2	Cr	O4	111.9(3)					
O3	Cr	O4	111.6(2)					

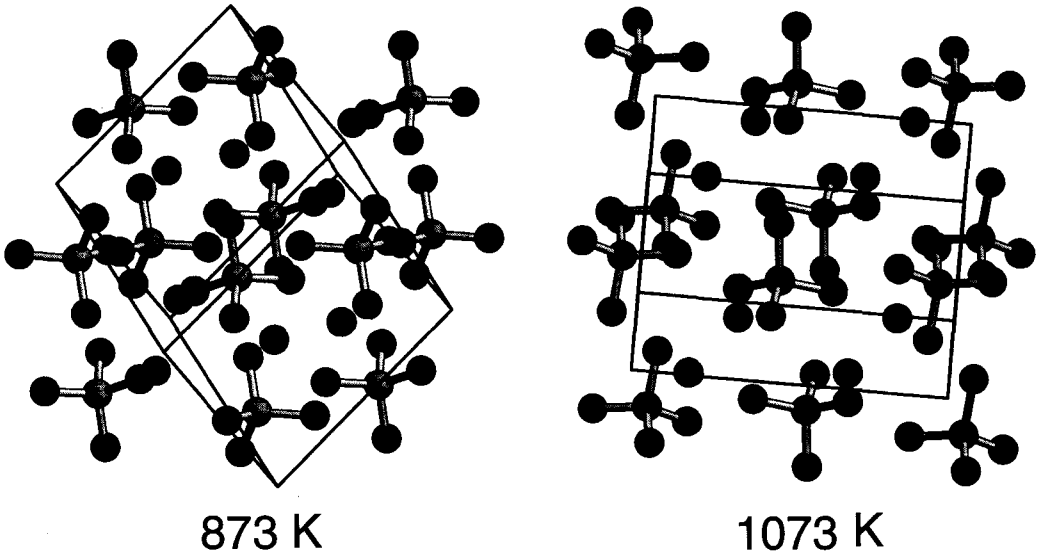

FIG. 5. Comparison of the crystal structures of crocoite at 873 and 1073 K. For the monazite structured phase at 873 K, [−0.544, −0.512, 0.665] is vertical and [0.668, −0.741, 0.071] is normal to the page. For the baryte structured phase at 1073 K, [−0.134, 0.922, 0.354] is vertical and [0.002, −0.362, 0.930] is normal to the page.

and Germs (1921) have measured an additional, lower temperature, probably second-order phase transition in pure $PbCrO_4$ which is apparently absent in the natural mineral we have studied. It is possible that the presence of low level impurities of Mo and S suppress this transition and a reinvestigation of synthetic and natural $PbCrO_4$ using DTA on either sealed samples or under controlled atmospheres could shed further light on this problem. From our earlier measurements on unsealed samples we conclude that it is probable that the diffraction patterns published by Pistorius and Pistorius on pure $PbCrO_4$ are simply decomposition products and do not represent the diffraction patterns of either an intermediate or an alternative high-temperature phase different to the baryte structured phase we have measured.

A high-temperature Raman study of a single crystal of crocoite from the batch examined in this study is due to be carried out shortly at the Risø National Laboratory in Denmark which hopefully will provide further information on the nature of the phase transition.

Acknowledgements

I am grateful to the following members of staff from the Department of Mineralogy at the Natural History Museum, London: Paul Schofield for arranging the microprobe analysis and commenting on an early draft of the manuscript; Peter Tandy for providing the specimen; and John Spratt for carrying out the chemical analysis. Duncan Francis of ISIS is thanked for preparing the furnace used in this study.

References

Brody, S.B. (1942) An X-ray investigation of the structure of lead chromate. *J. Chem. Phys.*, **10**, 650–2.

Collotti, G., Conti, L. and Zocchi, M. (1959) The structure of the orthorhombic modification of lead chromate $PbCrO_4$. *Acta Crystallogr.*, **12**, 416.

Ibberson, R.M., David, W.I.F. and Knight, K.S. (1992) The high resolution powder diffractometer (HRPD) at ISIS – a user guide. *Rutherford Appleton Laboratory Report* RAL-92-031.

Jaeger, F.M. and Germs, H.C. (1921) Über die binären systeme der sulfate, chromate, molybdate und wolframate des bleies. *Zeit. Anorg. Chem.*, **119**, 145–73.

Jessen, S.M. and Küppers, H. (1991) The precision of thermal-expansion tensors of triclinic and monoclinic crystals. *J. Appl. Crystallogr.*, **24**, 239–42.

Johnson, M.W. and David, W.I.F. (1985) HRPD: The high resolution powder diffractometer at the SNS. *Rutherford Appleton Laboratory Report* RAL-85-112.

Knight, K.S. (1996) A neutron powder diffraction determination of the thermal expansion tensor of crocoite ($PbCrO_4$) between 60 K and 290 K. *Mineral. Mag.*, **60**, 963–72.

Náray-Szabó I. And Argay, G. (1965) Die kristallstruktur des krokoites, $PbCrO_4$. *Acta Chimica Acad. Scientiarum Hungarae*, **40**, 283–8.

Parkes, G.D. (1952) *Mellor's comprehensive treatise on inorganic and theoretical chemistry, volume 11, revised edition*. Longmans, Green & Co.

Pawley, G.S. (1981) Unit cell refinement from powder diffraction scans. *J. Appl. Cryst.*, **14**, 357–61.

Pistorius, C.W.F.T. and Pistorius, M.C. (1962) Lattice constants and thermal-expansion properties of the chromates and selenates of lead, strontium and barium. *Zeits. Kristallogr.*, **117**, 259–71.

Popovkin, B.A. and Simanov, Yu.P. (1962) An X-ray diffraction study of the two modifications of lead selenate. *Zh. Neorgan. Khim.*, **7**, 1743–4.

Quareni S. and De Pieri, R. (1964) La struttura della crocoite, $PbCrO_4$. *Rend. Soc. Mineral. Italiana*, **20**, 253–250.

Quareni S. and De Pieri, R. (1965) A three-dimensional refinement of the structure of crocoite, $PbCrO_4$. *Acta Crystallogr.*, **19**, 287–9.

Quittner, F., Sagpir, J. and Rassudowa, N. (1932) Die rhombishe modifikation des bleichromates. *Zeit. Anorg. Chem.*, **204**, 315–7.

Schlenker, J.L., Gibbs, G.V. and Boisen, M.B. (1975) Thermal expansion coefficients for monoclinic crystals: a phenomenological approach. *Amer. Mineral.*, **60**, 828–33.

Wagner, H. (1931) Optische und röntgenographische untersuchen an pigmenten. *Zeit. Angew. Chem.*, **44**, 665–7.

Wagner, H., Haug, R. and Zipfel, M. (1932) Die modifikation des bleichromates. *Zeit. Anorg. Chem.*, **208**, 249–54.

[*Manuscript received 26 May 1999: revised 7 August 1999*]